Electron Cooling in a Magnetically Expanding Plasma

J. M. Little and E. Y. Choueiri
Electric Propulsion and Plasma Dynamics Laboratory (EPPDyL), Princeton University, Princeton, New Jersey, 08544, USA
(Received 22 September 2015; revised manuscript received 21 October 2016; published 23 November 2016)

Electron cooling in a magnetically expanding plasma, which is a fundamental process for plasma flow and detachment in magnetic nozzles, is experimentally investigated using a radio frequency plasma source and magnetic nozzle (MN). Probe measurements of the plasma density, potential, and electron temperature along the center line of the MN indicate that the expansion follows a polytropic law with exponent $\gamma_e = 1.15 \pm 0.03$. This value contradicts isothermal electron expansion, $\gamma_e = 1$, which is commonly assumed in MN models. The axial variation of the measured quantities can be described by a simple quasi-1D fluid model with classical electron thermal conduction, for which it has been previously shown that a value of $\gamma_e \approx 1.19$ is expected in the weakly collisional limit. A new criterion, derived from the model, ensures efficient ion acceleration when a critical value for the ratio of convected to conducted power is exceeded.

DOI: 10.1103/PhysRevLett.117.225003

The thermodynamics of an expanding magnetized plasma play an important role in momentum and energy transfer in the solar wind [1], astrophysical jets [2], and electric propulsion plasmas [3]. Electron cooling is especially important in electric propulsion concepts that rely on plasma acceleration through a magnetic nozzle (MN) [4] because momentum is primarily imparted to the thruster from the thermally expanding plasma propellant [5]. The commonly used assumption of isothermal expansion, often justified by referencing the large field-aligned electron thermal conductivity, leads to an exhaust jet with an unbounded kinetic power [6]. In spite of this physical inconsistency, isothermal models are useful for studying the macroscopic dynamics [7] of the expanding plasma and the influence of the plasma and magnetic field topologies [8]. The relevant physical processes in the downstream region, however, are strongly influenced by the electron temperature. Therefore, MN performance and plasma detachment models require improved understanding of electron cooling in magnetically expanding plasmas. In this Letter, we report our experimental measurements of the axial variation of the plasma parameters along the center line of a MN, demonstrate that the expansion follows a polytropic law, and compare the measured quantities to predictions from a quasi-1D analytical model that includes electron heat conduction along the magnetic field.

The plasma source (PS) [9] consists of a 7.5 cm inner diameter, 30.5-cm-long tube of borosilicate glass mounted concentrically inside two electromagnetic coils, each with a mean radius $r_c = 7.51$ cm. Argon gas is injected through the center of a Macor back plate located 18.5 cm upstream from the magnets. A two-turn spiral antenna positioned near the back plate is used to excite the plasma using 13.56 MHz rf radiation. The power delivered to the antenna was fixed at 500 W. The MN is formed by passing dc current through the electromagnets. The strength of the peak magnetic field, B_0, is controlled with the applied current, I_B, such that $B_0[\mathrm{G}] \approx 21 I_B[\mathrm{A}]$. Typical parameters within the PS are $n \sim 10^{18}$ m^{-3} and $T_e \sim 7$ eV, which are consistent with rf plasmas operating in the low-field helicon mode [10]. The PS is mounted inside a 2.4 m diameter × 7.6 m length fiberglass vacuum chamber (Fig. 1). The argon mass flow rate was held at 0.5 mg/s resulting in a chamber pressure of ~20 μTorr.

We characterized the expanding plasma using three diagnostics. A swept rf-compensated Langmuir probe (LP) [11] measured the plasma density n and electron temperature T_e. The probe's cylindrical tungsten electrode measured 0.25 mm in diameter and 3.0 mm in length, and was aligned with the flow direction to prevent distortion of the I-V curve [12]. The plasma potential, V_p, was measured using a heated emissive probe (EP) and the floating point method [13]. The EP filament was constructed of 0.125 mm diameter tungsten wire oriented perpendicular to the magnetic field [14]. Errors due to the formation of a double

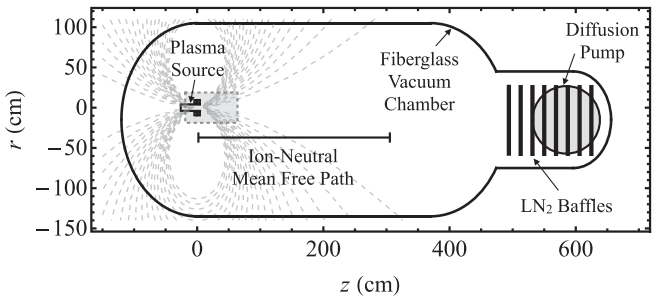

FIG. 1. Top-down diagram showing the approximate size and position of the plasma source and vacuum chamber. The gray box depicts the region shown in Fig. 2(a).

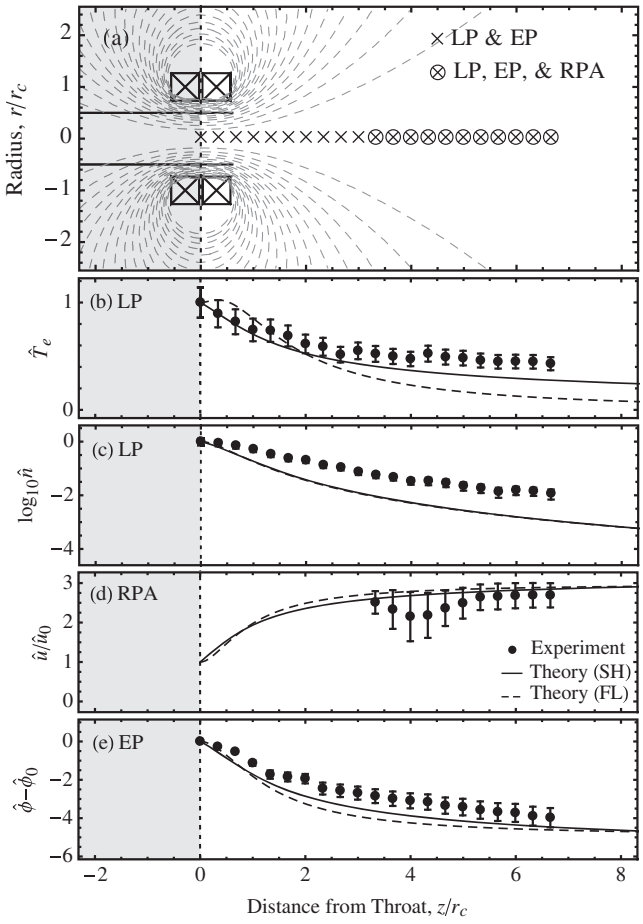

FIG. 2. (a) Schematic showing the plasma source, MN field lines (dashed) and measurement locations. The panels contain the following measurements for $I_B = 17.5$ A: (b) electron temperature, (c) plasma density, (d) mean ion velocity ($\hat{u}_0 \approx 1.12$), and (e) plasma potential. Solid and dashed lines in (b)–(e) represent theoretical predictions using the Spitzer-Harm (SH) and flux-limited (FL) models for electron heat conduction, respectively. The dotted line marks the location of the nozzle throat.

sheath were corrected for using $V_p = V_f^{\mathrm{em}} + 0.6T_e$ [15], where V_f^{em} is the floating potential of the emitting probe. We measured the ion energy distribution function (IEDF), $f_i(V)$, using a four-grid retarding potential analyzer (RPA) [16]. The ion beam voltage is calculated as $V_b = \int_0^{V_{\max}} f_i(V)VdV / \int_0^{V_{\max}} f_i(V)dV - V_p$, with V_p obtained from the EP. The mean ion velocity is $u = \sqrt{2eV_b/m_i}$, where e is the electron charge and m_i the ion mass. Data were acquired on time scales many orders of magnitude longer than the relevant plasma dynamic time scales and therefore only captures the time-averaged, steady-state behavior of the plasma.

Measurements were taken on the MN center line along which the magnetic field is purely axial [Fig. 2(a)]. Perturbations due to the size of the RPA restricted its use to $z \geq 25$ cm. Seven magnetic field strengths were investigated for $I_B \in [5, 20]$ A. The dependence of magnetic field strength on axial distance can be found in Ref. [9].

In Fig. 2 we show the axial variation of the measured plasma parameters. Normalized quantities are shown such that $\hat{n} \equiv n/n_0$, $\hat{T}_e \equiv T_e/T_{e,0}$, $\hat{u} \equiv u/\sqrt{T_{e,0}/m_i}$, and $\hat{\phi} \equiv V_p/T_{e,0}$, where the "0" subscript denotes values at $z = 0$. The distance from the throat is normalized by the magnet radius, r_c. It is evident that T_e decreases as the plasma expands through the diverging magnetic field. A supersonic ion beam forms downstream with an energy equal to the sum of the initial ion energy at the throat and the energy acquired through the ambipolar potential drop. This potential drop, formed to maintain quasineutrality in the exhaust, was observed to be the main source of ion acceleration in MN plasmas in which $T_e \gg T_i$ [17]. The large uncertainty in u around $z/r_c = 4$ is due to an anomalous broadening of $f_i(V)$ that appeared for some conditions [18]. The emissive probe measured plasma potential fluctuations of $\delta V_p/V_p \sim 0.2$ near the throat and $\delta V_p/V_p \sim 0.1$ in the plume—justifying the need for rf compensation of the LP.

In contrast to previous experiments on magnetically expanding plasmas, we did not detect slow ion and non-Maxwellian electron populations downstream. Slow ions, whose IEDF exhibits a peak near V_p, are created by ionization and charge-exchange of the background neutral gas [15,19,20]. For $n \sim 10^{18}$ m^{-3} and $T_e \sim 7$ eV the neutral mean free path for ionization is on the order of 10 cm near the MN throat [21]. Ionization of the background gas is negligible because the mean free path rapidly increases. Similarly, the ion mean free path for ion-neutral collisions is around 3 meters for a 20 μTorr background pressure [21]. The absence of a slow ion population in our experiment is consistent with the large collisional mean free paths relative to the expansion length scale. Analyzing our LP data using Drusteyev's method [22] we did not find evidence of high-energy electrons [23]. We note that although our LP followed established designs [11], it was not specifically engineered for high-resolution EEDF measurements [24], limiting our dynamic range to 2 orders of magnitude. It is possible that the high-energy tail occurs when electrons formed downstream via ionization or secondary electron emission from chamber walls acquire energy from the ambipolar electric field as they accelerate towards the PS. The absence of a measurable high-energy electron tail in our experiment may be due to the fact that both the distance to the chamber wall and neutral mean free path for ionization are much greater than the expansion length scale.

The polytropic state equation relates the pressure p and density n through the equation $p/n^\gamma = C(\psi)$. Here, γ is the polytropic index and C is constant along a characteristic surface ψ (e.g., a magnetic flux surface). For electrons, we calculate γ_e using linear regression of the $\log_{10} T_e$ vs $\log_{10} n$ and V_p vs T_e data sets [25], as shown in Figs. 3(a) and 3(b).

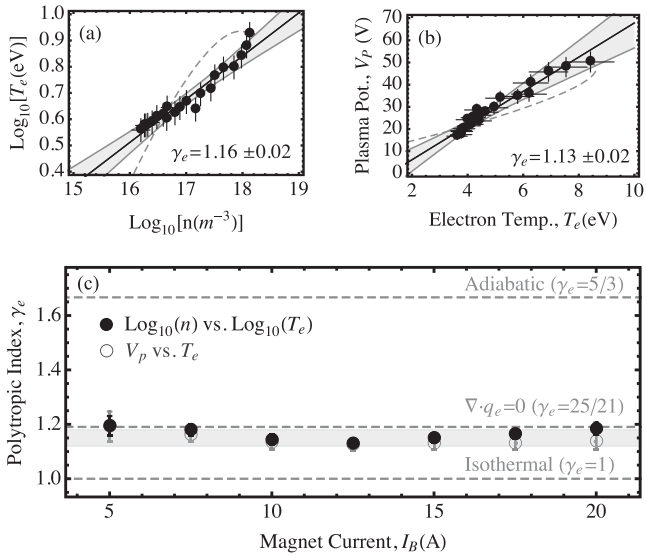

FIG. 3. Experimental measurements of (a) $\log_{10} T_e$ vs $\log_{10} n$, and (b) V_p vs T_e indicate that the expansion follows a polytropic law. The polytropic index is determined using the method of least squares (line). The 95% confidence interval is shown in gray. The solution to the quasi-1D model using FL electron heat conduction is also shown (dashed line). Using the results of two independent measurement methods, it is shown in (c) that the polytropic index is independent of the strength of the applied magnetic field. The shaded region in (c) corresponds to $\gamma_e = 1.15 \pm 0.03$.

The expansion follows a polytropic law as evidenced by the linear relationship between these data sets. Furthermore, the calculated γ_e agrees between the two independent methods to within experimental uncertainty. This agreement indicates that the EP and LP measurements are self-consistent—further implying Maxwellian electrons. These measurements also indicate for the first time that γ_e is largely unaffected by the applied magnetic field strength [Fig. 3(c)]. We calculate the weighted mean among all measurements to be $\gamma_e = 1.15 \pm 0.03$; a value that falls within isothermal and adiabatic expansion. It is interesting to note that similar values have been previously observed in the region of expanding solar wind [1] and the exhaust plume of Hall thruster plasmas [25,26].

These results contradict those of a similar study on a 30 kW MN plasma [27]. In the 30 kW study the authors infer $\gamma_e \approx 1.7$ from a T_e vs V_p data set and $\gamma_e \approx 3$ from a n vs V_p data set. Data were analyzed for 50 mg/s of argon flow, which resulted in a background pressure (100 μTorr) significantly larger than our experiments. In addition, the plasma source possessed physical walls that extended many plasma radii into the expansion region, increasing the local neutral density and impeding the free expansion of the plasma.

A recent experimental study [28] found a mechanism for electron cooling that is governed by collisionless electrons with a depleted high-energy population (resulting in a similar value of $\gamma_e = 1.17 \pm 0.02$). The authors show that a nonlocal, non-Maxwellian EEDF yields adiabatic cooling of an expanding electron population. In contrast to Ref. [28] where the densities were 2 orders of magnitude lower than reported here, frequent electron collisions produce a Maxwellian EEDF in our plasma source. Furthermore, downstream depletion of the high-energy population does not occur in our experiment because our vacuum chamber wall is nonconductive and located far from the plasma source. Therefore, collisionless electron cooling cannot explain the results reported here, and we seek an alternative justification for electron cooling in our MN.

Our experimentally derived value of γ_e is consistent with the value derived theoretically by Litvinov [29] in the limit where the flux of power from the MN is dominated by electron heat conduction along the magnetic field. Using a quasi-1D fluid model and assuming classical electron thermal conductivity, Litvinov shows that γ_e possesses a minimum value of $\gamma_{e,\min} \approx 1.19$. We now turn towards the quasi-1D model of Litvinov to understand the influence of a large electron heat flux on MN energy transfer in further depth.

Adopting the convention $y' \equiv dy/d\hat{z}$, the normalized plasma continuity and momentum equations are $(\hat{n}\,\hat{u}\,\hat{A})' = 0$ and $\hat{n}\,\hat{u}\,\hat{u}' + (\hat{n}\hat{T}_e)' = 0$. Electron pressure influences the ions through the ambipolar potential, $\hat{\phi}' = (\hat{n}\hat{T}_e)'/\hat{n}$. The omitted Lorentz force primarily governs cross-field confinement, and has negligible influence on field-aligned expansion [7]. In the above equations we have assumed $T_e \gg T_i$. Neglecting radiation the energy equation takes the form

$$[\hat{n}\,\hat{u}\,\hat{A}\,(\hat{u}^2/2 + 5\hat{T}_e/2) + \hat{q}_e\hat{A}/\mathrm{Nu}]' = 0. \qquad (1)$$

Here, q_e is the electron heat conduction and $\mathrm{Nu} \equiv n_0 T_{e,0}\sqrt{T_{e,0}/m_i}/q_{e,0}$ is the Nusselt number of the flow—a dimensionless parameter that compares the magnitude of convective to conductive heat transport, and as a consequence governs electron cooling in the fluid model.

$\mathrm{Nu} \ll 1$ implies $(\hat{q}_e\hat{A})' = 0$. Inserting the classical Spitzer-Harm (SH) [30] electron thermal conductivity and ignoring it's weak dependence on n and T_e (through the Coulomb logarithm) we obtain $\hat{A}\hat{T}_e^{5/2}\hat{T}_e' = (\hat{T}_e')_0$. The electron temperature gradient at the MN throat, $(\hat{T}_e')_0$, may be found from the requirement $\hat{T}_e \to 0$ as $\hat{z} \to \infty$. This yields, $(\hat{T}_e')_0 = -(2/7)\hat{k}_B^{-1}$, with $\hat{k}_B = \int_0^\infty \hat{A}^{-1} d\hat{z}$. Under these assumptions the energy equation is simply $\hat{T}_e^{7/2} = 1 - \hat{k}_B^{-1}\int_0^{\hat{z}} \hat{A}^{-1} d\hat{\zeta}$. Here, $\hat{\zeta}$ is the dummy variable for integration over $\hat{z}$. The equation for $\hat{T}_e$ is similar in form to the predicted T_e profile in the solar transition region [31]. Moreover, it shows that electron cooling occurs even in the limit of large field-aligned electron mobility. Electron cooling in this limit was also found in a theoretical

investigation of the influence of electron thermal energy on Hall thruster plume divergence [32].

We approximate the MN as a dipole, or $\hat{A} = (1+\hat{z}^2)^{3/2}$. The flow becomes choked when $\hat{A}' - \hat{T}_e^{-7/2}(\hat{T}_e')_0 = 0$. Here, $\hat{u}^* = (\hat{T}^*)^{1/2}$, where the asterisk denotes values at the location of the singularity, $\hat{z}^*$. It follows that $\hat{k}_B = 1$ and $(\hat{T}_e')_0 = -2/7$. The model accurately predicts the decrease of $\hat{T}_e$ with $\hat{z}$ in our plume [Fig. 2(b)]. The measured ambipolar potential drop and ion beam velocity also agree with the theoretical prediction [Figs. 2(d)–2(e)]. The discrepancy between the measured and predicted density [Figs. 2(c)] is due to the fact that ion cross-field motion produces a plume that is more focused towards the MN center line [7,33].

An alternative derivation for γ_e can found by noting that $\lim_{\hat{z}\to\infty}\hat{u}' = 0$. In this limit $\gamma_e = 1 - (\hat{T}_e')_0/\hat{\alpha}$, where $\hat{\alpha} = \lim_{\hat{z}\to\infty}(\hat{A}'\hat{T}_e^{7/2})$. The energy equation for $\mathrm{Nu} \ll 1$ gives $\hat{\alpha} = 3/2$, from which we find $\gamma_e = 25/21 \approx 1.19$.

Agreement between our experimental results and Litvinov's model for $\mathrm{Nu} \ll 1$ supports the theoretical scaling of SH conductivity. The SH model requires electron collisions to be frequent over the relevant length scale, or $\mathrm{Nu} \gg (m_e/m_i)^{1/2}$. When this condition is violated, a flux-limited model for electron heat conduction is often imposed in the form $q_{\mathrm{FL}} \equiv bnm_e v_{t,e}^3$, where $b \sim 10^{-2} - 1$ [34]. Taking $b = 0.01$ to match the downstream velocity to that of the SH model, we find the FL model to be in poor agreement with our experimental measurements (Figs. 2 and 3). A more rigorous solution [35] to the problem of collisionless plasma expansion using an electron kinetic model predicts polytropic scaling in only a limited region downstream from the MN throat, with a value $\gamma_e \approx 1.6$ predicted for argon [36]. For the sake of comparison, we calculate $\mathrm{Nu}_{\mathrm{SH}} = (5 \pm 2) \times 10^{-4}$ from our experimental data using SH thermal conductivity. Recognizing that the electron heat flux from the MN cannot exceed the power deposited into the plasma, we find the lower bound $\mathrm{Nu}_{\mathrm{min}} \approx 5 \times 10^{-3}$. Because $\mathrm{Nu}_{\mathrm{SH}} < \mathrm{Nu}_{\mathrm{min}}$ the effective electron thermal conductivity in our experiment must be at least an order of magnitude lower than predicted by the SH model. This disparity suggests an anomalously high electron collision rate—an inference that is further supported by the largely Maxwellian nature of our electrons and the strong disagreement between our experimental results and existing collisionless expansion models.

The results shown here raise an important fundamental question regarding the efficacy of MNs for plasma acceleration: is it possible to efficiently convert thermal energy into directed ion kinetic energy if the flux of power is dominated by electron heat conduction? To answer this question we look at the theoretical scaling of γ_e and η_{max} with Nu, shown in Fig. 4. Here, η_{max} is defined as the ratio of the ion kinetic power (as $\hat{z} \to \infty$) to the total power. Fig. 4(a) shows the expected transition between

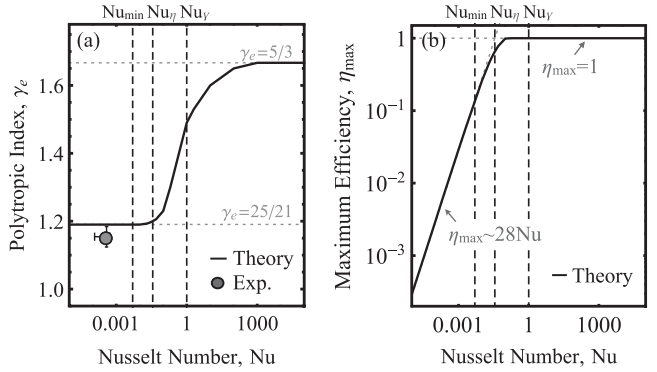

FIG. 4. Theoretical scaling of (a) γ_e vs Nu and (b) η_{max} vs Nu. The experimental data point in (a) represents the average value of γ_e obtained from Fig. 3(e) with Nu calculated using SH thermal conductivity. Power conservation sets the lower bound $\mathrm{Nu}_{\mathrm{min}}$.

conduction-dominated and adiabatic flow near $\mathrm{Nu}_\gamma \approx 1$. A similar transition occurs with η_{max} at a significantly lower value of $\mathrm{Nu}_\eta \approx 1/28$. Therefore, efficient ion acceleration is possible provided the ratio of convected to conducted power exceeds a critical value, defined by the criterion $\mathrm{Nu} \gtrsim \mathrm{Nu}_\eta$. The analytical expression for q_e as a function of γ_e used in some MN models [4] inherently assumes $\eta_{\mathrm{max}} = 1$ and only applies in the limit $\mathrm{Nu} \gg \mathrm{Nu}_\eta$. The potentially significant power loss due to unrecovered electron thermal energy for $\mathrm{Nu} < \mathrm{Nu}_\eta$ highlights a critical need for improved theoretical models of electron heat conduction in MNs.

[1] J. D. Scudder and S. Olbert, J. Geophys. Res. **84**, 6603 (1979).
[2] M. Birkinshaw, Astrophys. Space Sci. **242**, 17 (1996).
[3] E. Ahedo and J. Navarro-Cavallé, Phys. Plasmas **20**, 043512 (2013).
[4] M. Merino and E. Ahedo, IEEE Trans. Plasma Sci. **43**, 244 (2015).
[5] K. Takahashi, T. Lafleur, C. Charles, P. Alexander, and R. W. Boswell, Phys. Rev. Lett. **107**, 235001 (2011).
[6] H. Hügel, G. Krülle, and T. Peters, AIAA J. **5**, 551 (1967).
[7] E. Ahedo and M. Merino, Phys. Plasmas **17**, 073501 (2010).
[8] J. M. Little and E. Y. Choueiri, Phys. Plasmas **20**, 103501 (2013).
[9] J. M. Little and E. Y. Choueiri, IEEE Trans. Plasma Sci. **43**, 277 (2015).
[10] T. Lafleur, C. Charles, and R. W. Boswell, J. Phys. D **44**, 185204 (2011).
[11] I. D. Sudit and F. F. Chen, Plasma Sources Sci. Technol. **3**, 162 (1994).
[12] P. Chung, L. Talbot, and K. Touryan, Appl. Phys. Eng. **11** (1975).
[13] J. P. Sheehan and N. Hershkowitz, Plasma Sources Sci. Technol. **20**, 063001 (2011).
[14] S. Iizuka, P. Michelsen, J. J. Rasmussen, R. Schrittwieser, R. Hatakeyama, K. Saeki, and N. Sato, J. Phys. E **14**, 1291 (1981).

[15] L. T. Williams and M. L. R. Walker, IEEE Trans. Plasma Sci. **43**, 1694 (2015).
[16] J. D. Sommerville and L. B. King, J. Propul. Power **27**, 754 (2011).
[17] B. W. Longmier, E. A. Bering III, M. D. Carter, L. D. Cassady, W. J. Chancery, F. R. C. Díaz, T. W. Glover, N. Hershkowitz, A. V. Ilin, G. E. McCaskill *et al.*, Plasma Sources Sci. Technol. **20**, 015007 (2011).
[18] See Supplemental Material at http://link.aps.org/supplemental/10.1103/PhysRevLett.117.225003 for figures that show the axial evolution of the measured IEDF at different magnetic field strengths.
[19] C. Charles and R. W. Boswell, Phys. Plasmas **11**, 1706 (2004).
[20] A. Shabshelowitz and A. D. Gallimore, J. Propul. Power **29**, 919 (2013).
[21] G. Franz, *Low Pressure Plasmas and Microstructuring Technology* (Springer Science & Business Media, New York, 2009).
[22] A. Schwabedissen, E. C. Benck, and J. R. Roberts, Phys. Rev. E **55**, 3450 (1997).
[23] See Supplemental Material at http://link.aps.org/supplemental/10.1103/PhysRevLett.117.225003 for figures containing the EEPF obtained by applying Drusteyev's method to our Langmuir probe traces.
[24] V. Godyak and V. Demidov, J. Phys. D **44**, 233001 (2011).
[25] K. Dannenmayer and S. Mazouffre, Plasma Sources Sci. Technol. **22**, 035004 (2013).
[26] Y. Raitses, D. Staack, A. Smirnov, and N. Fisch, Phys. Plasmas **12**, 073507 (2005).
[27] J. P. Sheehan, B. W. Longmier, E. A. Bering, C. S. Olsen, J. P. Squire, M. G. Ballenger, M. D. Carter, L. D. Cassady, F. R. C. Díaz, T. W. Glover *et al.*, Plasma Sources Sci. Technol. **23**, 045014 (2014).
[28] Y. Zhang, C. Charles, and R. Boswell, Phys. Rev. Lett. **116**, 025001 (2016).
[29] I. I. Litvinov, J. Appl. Mech. Tech. Phys. **12**, 793 (1974).
[30] L. Spitzer Jr and R. Härm, Phys. Rev. **89**, 977 (1953).
[31] Ø. Lie-Svendsen, T. E. Holzer, and E. Leer, Astrophys. J. **525**, 1056 (1999).
[32] A. Cohen-Zur, A. Fruchtman, and A. Gany, IEEE Trans. Plasma Sci. **36**, 2069 (2008).
[33] J. M. Little, Ph.D. thesis, Princeton University, Princeton, NJ, 2015.
[34] R. Malone, R. McCrory, and R. Morse, Phys. Rev. Lett. **34**, 721 (1975).
[35] M. Martinez-Sanchez, J. Navarro-Cavallé, and E. Ahedo, Phys. Plasmas **22**, 053501 (2015).
[36] J. Navarro-Cavalle, S. Correyero, and E. Ahedo, *Proceedings of 34th International Electric Propulsion Conference, Kobe, Japan, July 4–10, 2015*, IEPC-2015-117 (IEPC, Kobe, 2015).